

Research



Cite this article: Chang M *et al.* 2017 Region-specific RNA m⁶A methylation represents a new layer of control in the gene regulatory network in the mouse brain. *Open Biol.* **7**: 170166.
<http://dx.doi.org/10.1098/rsob.170166>

Received: 6 July 2017
Accepted: 9 August 2017

Subject Area:
genomics/neuroscience

Keywords:
N⁶-methyladenosine, RNA methylation, mouse cerebellum, mouse cerebral cortex, epitranscriptomic mark

Authors for correspondence:
Yamei Niu
e-mail: niuyam@ibms.pumc.edu.cn
Wei-Min Tong
e-mail: wmtong@ibms.pumc.edu.cn

[†]These authors contributed equally to the paper as joint first authors.

Electronic supplementary material is available online at <https://dx.doi.org/10.6084/m9.figshare.c.3863188>.

Region-specific RNA m⁶A methylation represents a new layer of control in the gene regulatory network in the mouse brain

Mengqi Chang^{1,†}, Hongyi Lv^{2,3,†}, Weilong Zhang⁴, Chunhui Ma¹, Xue He¹, Shunli Zhao¹, Zhi-Wei Zhang¹, Yi-Xin Zeng⁴, Shuhui Song², Yamei Niu¹ and Wei-Min Tong¹

¹Department of Pathology, Institute of Basic Medical Sciences and Neuroscience Center, Chinese Academy of Medical Sciences and Peking Union Medical College, Beijing 100005, People's Republic of China

²BIG Data Center, Beijing Institute of Genomics, Chinese Academy of Sciences, Beijing 100101, People's Republic of China

³University of Chinese Academy of Sciences, Beijing 100049, People's Republic of China

⁴State Key Lab of Molecular Oncology, National Cancer Center/Cancer Institute and Hospital, Chinese Academy of Medical Sciences and Peking Union Medical College, Beijing 100021, People's Republic of China

ORCID iD: SS, 0000-0003-2409-8770; YN, 0000-0003-2078-0780; W-MT, 0000-0002-6240-0267

N⁶-methyladenosine (m⁶A) is the most abundant epitranscriptomic mark found on mRNA and has important roles in various physiological processes. Despite the relatively high m⁶A levels in the brain, its potential functions in the brain remain largely unexplored. We performed a transcriptome-wide methylation analysis using the mouse brain to depict its region-specific methylation profile. RNA methylation levels in mouse cerebellum are generally higher than those in the cerebral cortex. Heterogeneity of RNA methylation exists across different brain regions and different types of neural cells including the mRNAs to be methylated, their methylation levels and methylation site selection. Common and region-specific methylation have different preferences for methylation site selection and thereby different impacts on their biological functions. In addition, high methylation levels of fragile X mental retardation protein (FMRP) target mRNAs suggest that m⁶A methylation is likely to be used for selective recognition of target mRNAs by FMRP in the synapse. Overall, we provide a region-specific map of RNA m⁶A methylation and characterize the distinct features of specific and common methylation in mouse cerebellum and cerebral cortex. Our results imply that RNA m⁶A methylation is a newly identified element in the region-specific gene regulatory network in the mouse brain.

1. Background

N⁶-methyladenosine (m⁶A) is a reversible mRNA epigenetic mark that has been shown to regulate RNA metabolism or structure by either facilitating or preventing methylation-dependent RNA–protein interaction [1–3]. An increasing body of evidence indicates that m⁶A methylation of nuclear mRNAs regulates pre-mRNA splicing [4,5], nuclear export [6] and pri-miRNA processing [7,8], while cytoplasmic methylated mRNAs are involved in translational control [9–15] and mRNA decay [16,17].

The importance of m⁶A in diverse biological processes has been investigated mainly through modulating the expression of m⁶A-related genes [18,19]. It was reported in yeast, *Arabidopsis*, zebrafish and *Drosophila* that m⁶A methyltransferases METTL3 and WTAP are essential for meiosis, development and viability [19–24]. In mammalian cells, both METTL3 and METTL14 are important for

self-renewal and differentiation of mouse embryonic stem cells [24–29]. In addition, silencing of METTL3 led to circadian period elongation in mice [30]. RNA demethylase Alkbh5-deficient male mice showed defective spermatogenesis due to an imbalance in m⁶A levels [6]. Another RNA demethylase, FTO, is abundant in the brain and plays a regulatory role in adipogenesis, dopaminergic signalling and adult neurogenesis [31–35].

Like all physiological processes, neural activities rely on precise regulation of gene expression programmes at both genetic and epigenetic levels [36]. Epigenetic control of neurogenesis has been intensively investigated, with mechanisms including DNA methylation [37], histone modification [38], chromatin remodelling [39] and non-coding RNAs (lncRNAs) [40]. RNA modifications such as m⁶A, 5-methylcytidine (m⁵C) and N¹-methyladenosine (m¹A) have been proved to be essential regulatory elements in various biological processes [41–45]. Given a growing population of coding and lncRNAs identified in the brain, RNA modifications are thought to be important epitranscriptomic marks in the brain [46]. m⁶A was found to be dynamically regulated during brain development and correlated with memory formation [34,35,47,48]. However, despite the numerous experimental findings, the precise biological functions of m⁶A in the brain still await elucidation. Meanwhile, the brain is unique in its anatomical complexity and cellular heterogeneity [36,49,50], necessitating a detailed investigation into the regulatory role of m⁶A in the brain.

To explore the functional relevance of region-restricted m⁶A methylation in different brain regions, we performed the first transcriptome-wide m⁶A profiling analysis using adult mouse cerebellum and cerebral cortex.

2. Methods

2.1. Animals

All experiments were performed using wild-type, two-month-old C57/BL6 mice purchased from Vital River Co. (Beijing, China). All animal experiments and euthanasia were approved and performed in accordance with the guidelines of Animal Care and Use Committee of IBMS/PUMC.

2.2. RNA isolation

Mice were euthanized by cervical dislocation, and their cerebellum and cerebral cortex were dissected as described previously [51]. Mouse tissues were immediately snap-frozen into liquid nitrogen and then stored at –80°C until further use. Total RNA and poly(A) RNA were purified from frozen mouse cerebellum or cerebral cortex using TRI-Reagent (SIGMA) and FastTrack[®] MAG mRNA Isolation Kits (LIFE). Poly(A) RNA purity was confirmed by using Agilent Bioanalyzer 2100. When needed, the poly(A) RNA will be purified again using the RiboMinus[™] Human/Mouse Transcriptome Isolation Kit (LIFE).

RNA expression of m⁶A writers and erasers in the cerebellum and the cerebral cortex was measured by reverse transcription (TOYOBO) of total RNA and subsequent quantitative real-time PCR (TOYOBO). *Gapdh* was used as an

internal control. The primers used in this study are listed in the electronic supplementary material, table S12.

2.3. Quantitative m⁶A level measurement using UHPLC-MS/MS

The global m⁶A methylation level of poly(A) RNA was measured using Agilent Technologies 6490 Triple Quadrupole LC/MS as described before [6]. Briefly, RNA was digested with nuclease P1 (Sigma) at 37°C for 2 h, followed by treatment with calf intestine alkaline phosphatase (CIAP, Promega) at 37°C for 2 h. The solution was filtered and injected into the UHPLC-MS/MS system. The absolute m⁶A level in each sample was calculated by comparison with the standard curve obtained from pure nucleoside standards loaded simultaneously. The ratio of m⁶A to A was calculated to reflect the global methylation level.

2.4. Western blot analysis

Mouse cerebellum and cerebral cortex were dissected as described above and triturated in RIPA buffer supplemented with protease and phosphatase inhibitors; 60–80 µg of tissue lysates were subjected to SDS-PAGE and western blot analysis. Primary antibodies used in our analysis are as follows: anti-METTL3 (Abnova, H00056339-B01P), anti-METTL14 (Atlas Antibodies, HPA038002), anti-ALKBH5 (Sigma, HPA007196), anti-WTAP (Santa Cruz, sc-55438), anti-FTO (Abcam, ab92821) and beta-ACTIN (Santa Cruz, sc-47778). Secondary antibodies used are as follows: peroxidase-conjugated AffiniPure Goat Anti-Rabbit IgG (H + L) (XiYA Biology, Beijing, FZ-4201), peroxidase-conjugated AffiniPure Goat Anti-Mouse IgG (H + L) (XiYA Biology, Beijing, FZ-4202) and peroxidase-conjugated AffiniPure Rabbit Anti-Goat IgG (H + L) (XiYA Biology, Beijing, FZ-4203).

2.5. Immunohistochemical analysis

After being euthanized with tribromoethanol solution (4 mg g⁻¹), mouse whole brain was dissected and post-fixed in 4% paraformaldehyde overnight at 4°C. Subsequently, the brain was dehydrated with ethanol, clarified with xylene and then embedded in paraffin. Sections 4 µm thick were used for immunostaining. Primary antibodies used in the analysis included: anti-METTL3 (Proteintech, 15073-1-AP), anti-METTL14 (Atlas Antibodies, HPA038002), anti-WTAP (Proteintech, 60188-1-IG), anti-ALKBH5 (Sigma, HPA007196) and anti-FTO (Abcam, AB92821). Secondary antibodies included: ImmPRESS Anti-Mouse Ig (peroxidase) Kit (Vector, MP-7402) and ImmPRESS Anti-Rabbit Ig (peroxidase) Kit (Vector, MP-7401). Staining of brain sections was visualized using a Panoramic MIDI II digital slide scanner (3D HISTECH).

2.6. m⁶A-immunoprecipitation

For each m⁶A-immunoprecipitation (IP) reaction, cerebellar RNA was pooled from three male and three female mice, while cortical RNA was pooled from one male and one female mouse. Poly(A) RNA fragmentation was performed using RNA Fragmentation Reagents (Ambion) as instructed by the manufacturer. Five micrograms of fragmented

poly(A) RNA was incubated with 12.5 μg of anti-m⁶A antibody (Synaptic System) at 4°C for 2 h, followed by addition of protein A-Sepharose 4B (Sigma). After overnight incubation at 4°C, beads were washed five times with IPP buffer (150 mM NaCl, 0.1% NP-40, 10 mM Tris-HCl, pH 7.4). Immunoprecipitated RNA was recovered by competitive elution with m⁶A and subsequent ethanol precipitation. Input and immunoprecipitated RNA products were used for cDNA library construction using the TruSeq RNA Sample Prep Kit protocol (Illumina), and were subjected to a 2 \times 100 paired-end sequencing run using the Illumina HiSeq 3000 system. Two sets of biological replicates were performed to obtain reproducible results.

2.7. Data processing and reads mapping

For each sample, single-end reads (R2) were used for bioinformatic analysis. The quality control of raw data was evaluated using the FASTQC software (v. 0.10.1). Sequencing data were preprocessed with in-house Perl scripts following three criteria: (i) the adaptor sequence was removed by finding the sequence GATCGGAAGA with at most two mismatched bases; (ii) the read bases with low quality score (less than 20) were trimmed off from the 3'-end; (iii) the reads longer than 20 nt and with high quality score (more than 70% bases with quality score greater than 25) were retained. The filtered reads longer than 50 nt were mapped against the mouse genome (mm10), allowing up to two mismatches using the TOPHAT software (v. 2.0.13) [52,53]. Only uniquely mapped reads were kept for the downstream analysis.

2.8. RNA expression analysis

Fragments per kilobase of transcript per million mapped read (FPKM) values for each gene in the cerebellum and the cortex were calculated by the CUFFLINKS toolkit (v. 2.0.2) [54]. Two biological replicates of each sample were combined for calculating FPKM. Transcripts with FPKM value larger than 0.2 were considered as stably expressed transcripts [55].

2.9. M⁶A peak calling and motif analysis

M⁶A peak calling was performed using the EXOMEPEAK software (v. 2.7.0) with a cut-off of the false discovery rate (FDR) less than 5% [56,57]. Only the m⁶A peaks having an overlap (greater than 50% in length) between the two replicates are considered as concordant m⁶A peaks and are used for the subsequent analysis intersectBed from BEDTOOLS (v. 2.26.0) [58]. The common and specific m⁶A peaks were defined using the following criteria: (i) the common m⁶A peaks appear in the two biological replicates in both the cerebellum and the cortex; (ii) the specific m⁶A peaks appear in the two biological replicates of the cerebellum or the cortex, but not in any replicate of the other brain region. Commonly methylated mRNAs (CMRs) were defined as mRNAs containing common m⁶A peaks, while specifically methylated mRNAs (SMRs) were defined as mRNAs containing specific m⁶A peaks. Consensus sequence motifs enriched in m⁶A peaks were identified by HOMER [59]. To verify the results obtained using the EXOMEPEAK software, peak calling analysis was also performed in parallel using the MACS software with the default parameters [60,61].

2.10. Characterization of m⁶A peak distribution patterns

The distribution of m⁶A peaks were characterized as previously described with minor modification [27,62]. A mouse reference transcriptome was generated first by using the longest transcript for each gene to characterize the distribution patterns of m⁶A peaks. For each transcript of protein-coding genes, 100 bins of equal length were split for the 5'UTR, coding sequence (CDS) and 3'UTR, respectively. For long non-coding RNA (lncRNA), the entire length of lncRNA was split into 100 bins with equal length. The percentage showing the number of m⁶A peaks in each bin is calculated to represent the occupancy of m⁶A peaks along the whole transcript.

To determine the distribution of m⁶A peaks, we divided the longest transcript of protein-coding genes into five regions, namely the 5'UTR region, start codon region, CDS region, stop codon region and 3'UTR region. For those transcripts with a 5'UTR or 3'UTR longer than 100 nt and a CDS longer than 200 nt, a 200 nt region centred on start codons or stop codons was defined as start codon region or stop codon region. For the transcripts whose 5'UTR or 3'UTR was shorter than 100 nt, the corresponding UTR regions were classified as start codon regions or stop codon regions. If the entire length of the CDS was less than 200 nt, the first half of the CDS was classified as the start codon region and the remaining sequence as the stop codon region. The m⁶A peaks of both the cerebellum and the cortex were mapped to each region using intersectBEDTOOLS. If one m⁶A peak was mapped to more than one region, the priority of classification was set in the following order: (1) stop codon region, (2) start codon region, (3) CDS region, (4) 3'UTR region and (5) 5'UTR region. The number of m⁶A peaks in each region was calculated using the method described above.

2.11. Gene Ontology analysis

The DAVID tool with default parameters was used for Gene Ontology (GO) analysis [63]. Enriched GO terms shown in the main figures were manually curated, and a list of all selected terms of the biological process, cellular components and molecular functions category are provided in the electronic supplementary material tables.

2.12. Statistical analysis

Two-tailed Student's *t*-test was performed for statistical analysis of results in LC/MS and real-time qPCR. The Wilcoxon test was used for all bioinformatic analysis.

3. Results

3.1. Ubiquitous expression of m⁶A writers and erasers in mouse cerebellum and cerebral cortex

To obtain a complete view of m⁶A RNA methylation profiles from different tissues, we quantified the m⁶A content in various adult mouse tissues using an UHPLC-MS/MS assay. Although m⁶A was present in all tested tissues, RNA methylation levels were the highest in the brain (electronic supplementary material, figure S1a). In agreement with the

structural complexity in the brain, RNA methylation levels in the brainstem, olfactory bulb, cortex, cerebellum and thalamus varied from each other. In this study, we chose mouse cerebellum and cerebral cortex for all subsequent analysis.

To gain a better understanding of the regional regulation of m⁶A methylation, we examined the expression profiles of five methyltransferases and demethylases: METTL3, METTL14, WTAP, ALKBH5 and FTO (figure 1*a* and electronic supplementary material, figure S1*b*). Notably, both protein and RNA expression levels of methyltransferases and demethylases appeared to be higher in the cerebellum than those in the cerebral cortex. To examine the *in situ* protein expression, we performed immunohistochemical staining. As shown in figure 1*b*, all five proteins were readily detected in the molecular layer (ML), Purkinje cells layer (PCL) and internal granular layer (IGL) of the mouse cerebellum, albeit with varying staining intensities. Similarly, all five proteins were ubiquitously expressed in the cerebral cortex with different levels among each layer (figure 1*c*). The ubiquitous expression of these proteins indicated that m⁶A methylation plays a role in various types of neural cells.

3.2. Distinct m⁶A methylation patterns between mouse cerebellar and cerebral cortical RNAs

To assess whether m⁶A methylation represents an important epigenetic mark in the mouse cerebellum and cerebral cortex, we conducted a transcriptome-wide m⁶A-seq analysis separately. Concordant m⁶A peaks from the two biological replicates were used for subsequent bioinformatic analysis (figure 2*a,b*, electronic supplementary material, table S1).

Although similar numbers of mRNAs were expressed (figure 2*c*; electronic supplementary material, table S2), the absolute numbers of methylated mRNAs and methylation sites were higher in the cerebellum than in the cortex (electronic supplementary material, table S3; figure 2*d,e*). Comparison between the two brain regions revealed the existence of both CMRs and SMRs (figure 2*d*, electronic supplementary material, figure S3 and table S3). In spite of the lower numbers of specifically expressed mRNAs in the cerebellum (426) than in the cortex (849) (figure 2*c*, electronic supplementary material, table S2), the number of SMRs was much higher in the cerebellum (1559) than in the cortex (712) (figure 2*d*, electronic supplementary material, table S3). Consistently, cerebellar mRNAs had more specific methylation sites than cortical mRNAs (figure 2*e*). Among these SMRs, only a few were specifically expressed (three specifically expressed genes in the cerebellum and one in the cortex), implying that RNA methylation constitutes an additional layer of regulation in a region-specific manner. Furthermore, the methylation levels between the cerebellum and the cortex were compared. As shown in figure 2*f,g*, the cerebellar mRNAs had significantly higher methylation levels than cortical mRNAs at both peak levels and gene levels (electronic supplementary material, figure S2*a* & S2*b*). Compared with the SMRs, the CMRs contained more peaks with higher fold enrichment (figure 2*h*, electronic supplementary material, figure S2*c*, S2*d*, and table S3), resulting in a more significant difference in methylation levels between CMRs and SMRs (figure 2*i*, electronic supplementary material, figure S2*e*, S2*f*). Considering that the largely different numbers of CMRs and SMRs may generate

a difference when comparing their methylation levels, we randomly extracted the same numbers of peaks or RNAs from CMRs for a total of 10 times, which also showed significantly higher fold enrichment than those of SMRs (electronic supplementary material, figure S2*g*, S2*h*).

Considering the biological importance of lncRNAs in the brain, we also analysed the methylation profiles of lncRNAs in the two brain regions. The proportion of methylated lncRNAs, as well as the average number of m⁶A peaks per transcript, was much lower than those of methylated mRNAs (electronic supplementary material, table S2 and S3). As shown in the electronic supplementary material, figure S4*a* and S4*b*, in spite of comparable numbers of lncRNAs detected in the two brain regions, the cerebellum contained more methylated lncRNAs than the cortex samples. However, the proportion of specifically methylated lncRNAs was higher than those of mRNAs, suggesting that to exert their functions, lncRNAs exhibit a higher requirement for brain region-specific methylation (electronic supplementary material, figure S4*b*). The common and specific m⁶A methylation of lncRNAs in both regions were visualized from several randomly selected lncRNAs including *Malat1*, *Dlx4os* and *Miat* (electronic supplementary material, figure S4*c*).

We next evaluated how RNA methylation had an impact on RNA expression by using the input sample from the same experiment. We found that the median expression levels of methylated mRNAs were much higher than those of non-methylated mRNAs (electronic supplementary material, figure S5*a*). However, among all the methylated mRNAs, we observed a negative correlation between RNA abundance and RNA methylation levels (electronic supplementary material, figure S5*b,S5c*). Interestingly, the RNA abundance of the CMRs was significantly higher than that of SMRs in both the cerebellum and the cerebral cortex (electronic supplementary material, figure S5*d*).

Taken together, this comparative analysis revealed that the methylation levels of cerebellar RNAs were higher than those of cortical RNAs. CMRs and SMRs differed from each other in their methylation levels and overall RNA abundance, suggesting that common and specific methylation regulate gene expression in different ways.

3.3. Different distribution patterns between common and specific m⁶A peaks

In most cases, m⁶A methylation does not occur randomly along the transcript but at specific consensus sequences and enrichment sites. To test whether this characteristic also exists in cerebellar and cortical RNAs, we performed a motif-searching analysis with all m⁶A peaks and found that GGACU/UGGAC were the most conserved consensus motifs in both the cerebellum and the cortex (figure 3*a*, electronic supplementary material, figure S6*a–d*).

We next analysed the distribution patterns of m⁶A peaks along the transcript. In addition to previously reported enrichment sites in the stop codon, a pronounced enrichment was also found surrounding the start codons in both the cerebellum and the cortex (figure 3*b*, electronic supplementary material, figure S6*e*). Common m⁶A peaks exhibited similar distribution patterns because they accounted for more than 75% of m⁶A peaks (figure 3*c*; electronic supplementary

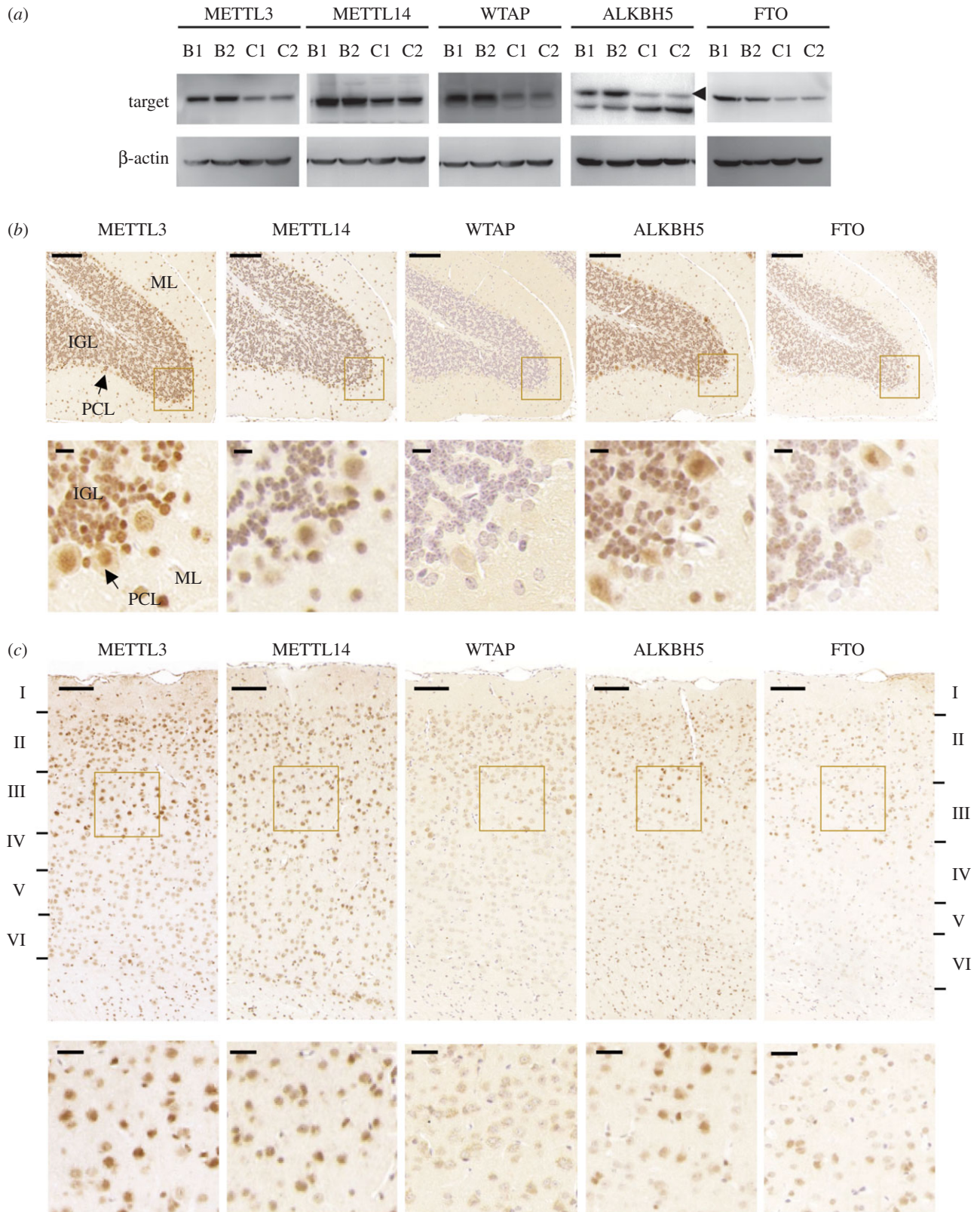


Figure 1. Protein expression of m⁶A writer and eraser genes in adult mice cerebellum and cerebral cortex. (a) Western blot analysis of METTL3, METTL14, WTAP, ALKBH5 and FTO in adult mouse cerebellum (B1, B2) and cerebral cortex (C1, C2). Beta-actin was used here as an internal control. Experiments were performed in biological triplicates using six mice in total. Representative results are shown here. (b,c) Representative images of immunostaining of METTL3, METTL14, WTAP, ALKBH5 and FTO using paraffin sections of adult mice cerebellum (b) and cerebral cortex (c). ML, molecular layer; IGL, inner granule cell layer; PCL, Purkinje cell layer. Scale bars represent 200 μ m. The laminar structure of the cortex was labelled from layer I to layer VI. Experiments were performed in biological triplicates using three male and three female mice in total and representative data are given here. Enlarged images in the square area are shown in the lower panels and scale bars represent 10 μ m in (b) and 50 μ m in (c).

material, table S4 and S5). In those cerebellum-specific methylated transcripts, more m⁶A peaks were detected in the vicinity of start codons rather than stop codons. By

contrast, cortex-specific m⁶A peaks were located near start codons and stop codons, as well as in the CDS (figure 3d, electronic supplementary material, table S6 and S7). To

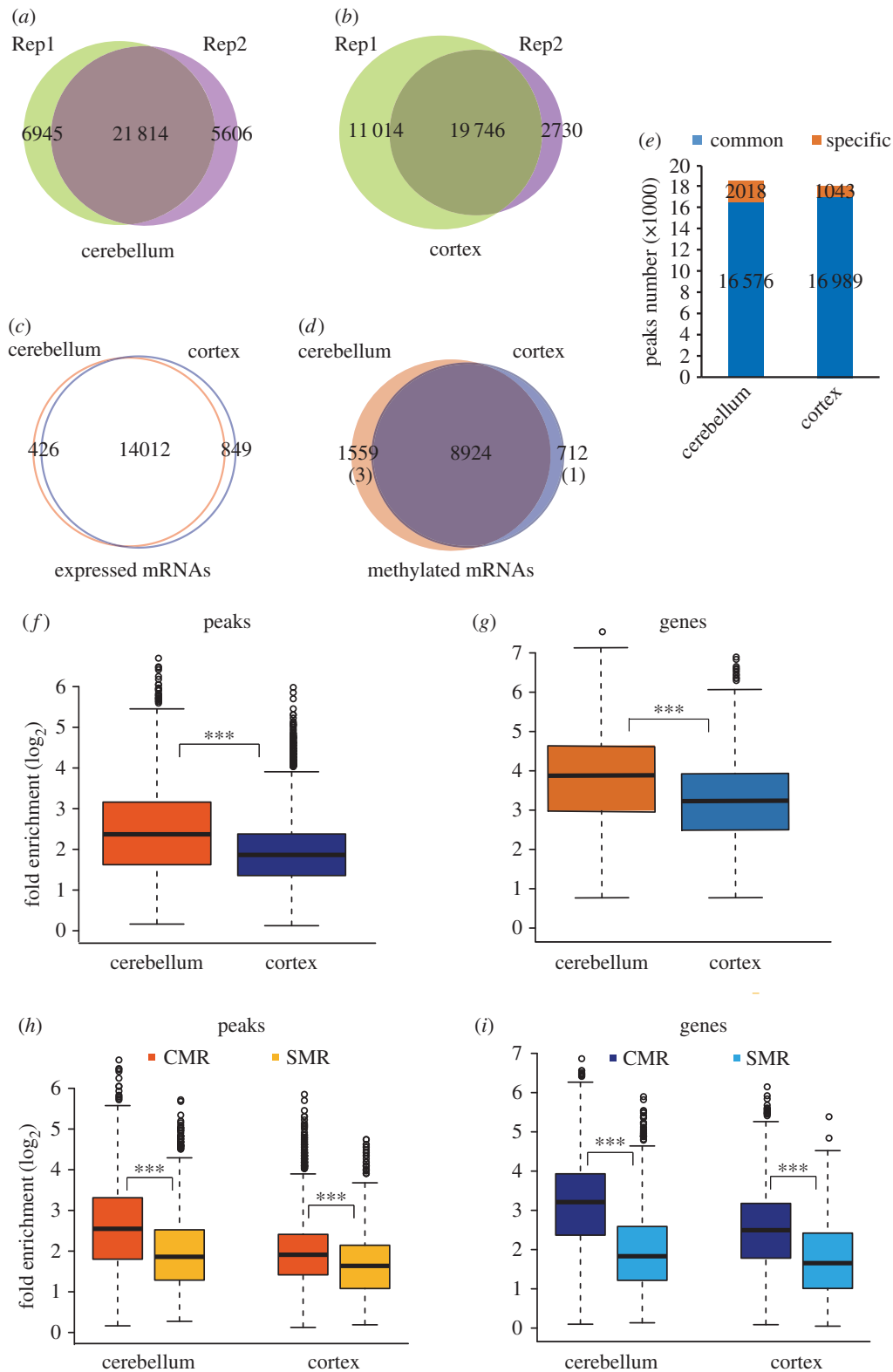


Figure 2. Region-specific m⁶A methylation in the mouse cerebellum and cerebral cortex. (a, b) Venn diagrams showing the numbers of overlapping m⁶A transcripts in the two biological replicates of m⁶A-IP in the cerebellum (a) and the cerebral cortex (b). (c) Venn diagram showing the numbers of genes commonly or specifically expressed in the cerebellum or the cerebral cortex. (d) Venn diagram showing the numbers of CMRs and SMRs. Numbers of specifically expressed genes among SMRs are shown in parentheses. (e) Column chart showing the numbers of common and specific m⁶A peaks in mouse cerebellum and cerebral cortex. The blue bars indicate common peaks, while the orange bars indicate specific peaks. (f, g) Box plots showing the methylation levels of cerebellar RNAs and cortical RNAs by comparing the median fold enrichment at peak levels (f) and gene levels (g). (h, i) Box plots showing the methylation levels of CMRs and SMRs by comparing the fold enrichment at the peak level (h) or gene level (i). Wilcoxon test was performed for statistical analysis. ****p* value < 2.2 × 10⁻¹⁶.

investigate the distribution patterns of common and specific peaks in detail, we analysed the peak numbers enriched in each gene region between the cerebellum and the cortex

(figure 3e). When taking all the methylation sites into consideration, m⁶A sites were most abundant near stop codons and the 3'UTR, which was similar to previous reports.

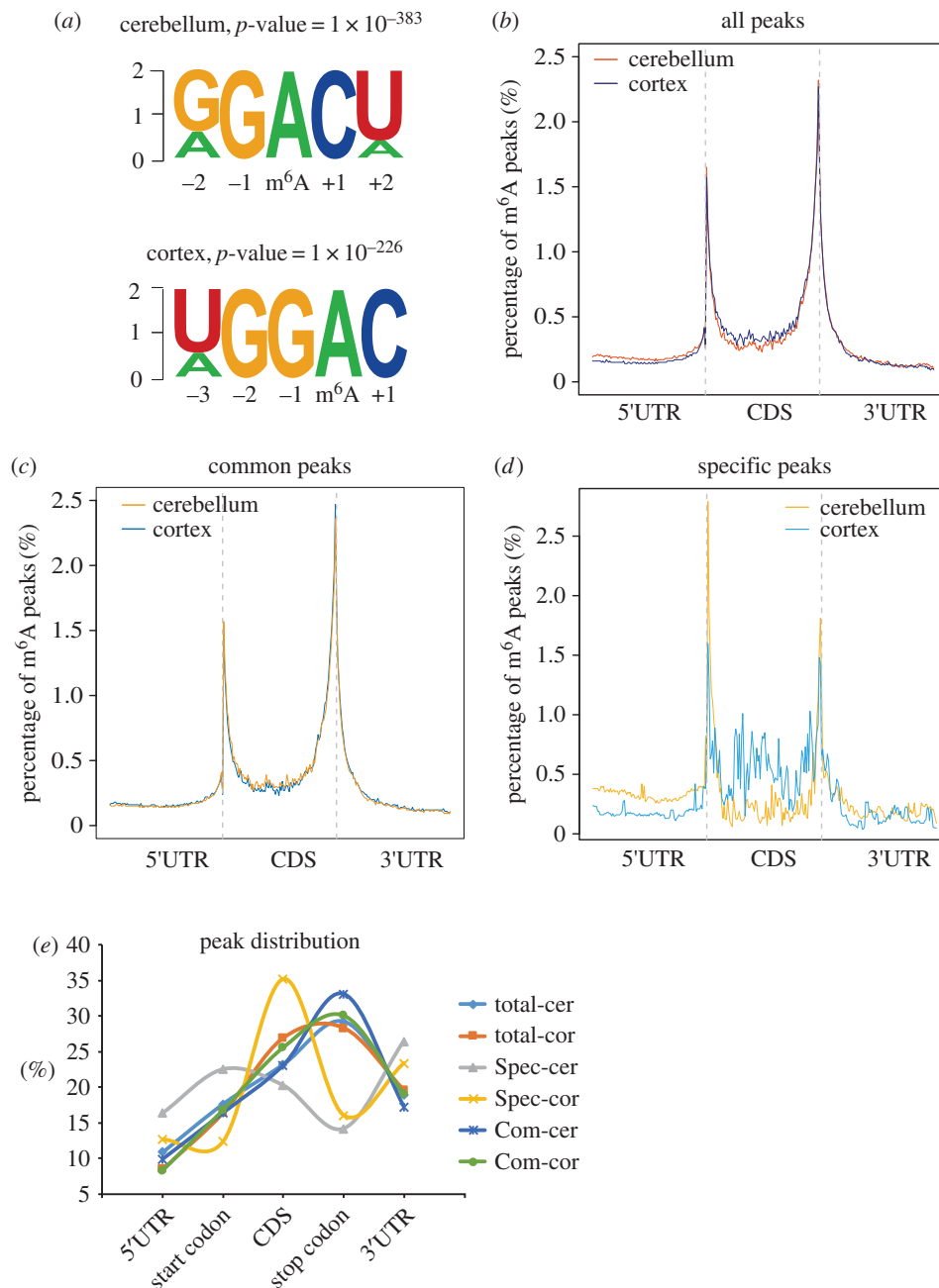


Figure 3. Distribution patterns of m⁶A peaks in mouse cerebellar and cerebral cortical mRNAs. (a) Sequence logo representing the deduced consensus motif through clustering of all enriched m⁶A peaks in the cerebellum and the cerebral cortex. (b–d) Enrichment of all m⁶A peaks (b), common m⁶A peaks (c) and specific m⁶A peaks (d) along the whole mRNA transcripts. (e) Statistics of numbers of m⁶A peaks enriched in different regions along the mRNA transcripts. Total m⁶A peaks in the cerebellum (total-cer) and cortex (total-cor); specific m⁶A peaks in the cerebellum (Spec-cer) and cortex (Spec-cor); common m⁶A peaks in the cerebellum (Com-cer) and cortex (Com-cor) were included and compared.

Notably, common and specific m⁶A peaks exhibited very different distribution patterns. The common m⁶A peaks were predominantly distributed near stop codons and the 3'UTR. By contrast, cerebellum-specific peaks were mainly distributed in start codons and 3'UTR regions, whereas cortex-specific peaks were mainly distributed in the CDS region.

In addition to m⁶A, N⁶, 2'-O-dimethyladenosine (m⁶Am) is another RNA modification found at the first nucleotide downstream from the m⁷G cap in the 5'UTR of mRNAs [64]. As the anti-m⁶A antibody has a cross-reactivity with m⁶Am, the length of the 5'UTR was calculated to test if the m⁶A observed at the start codon was due to the presence of m⁶Am. Among CMRs and cortical SMRs that contained m⁶A peaks surrounding start codons, more than 70% of them had a 5'UTR longer than 100 nt, while 60% of cerebellar SMRs had a 5'UTR longer

than 100 nt (electronic supplementary material, figure S6f). Furthermore, m⁶Am was detected in only 30% of mRNA caps with a ratio of m⁶A to m⁶Am of approximately 30 [65]. Thus, the methylation sites surrounding start codons in our study are most probably m⁶A, rather than m⁶Am. However, for those methylated transcripts with a 5'UTR shorter than 100 nt, single-nucleotide resolution analysis should be performed to distinguish between m⁶A and m⁶Am [66].

3.4. Higher m⁶A methylation levels in neurons than in glial cells among the cell type-enriched RNAs

The mammalian brain is the most sophisticated organ ever studied, exhibiting considerable structural complexity and

cellular diversity. With the discovery of additional epigenetic marks on mRNA, characterization of their functions in different cell types is essential for a more detailed understanding of the intricate mechanisms governing the brain functions. However, the current m⁶A-seq analysis is unable to discriminate RNA methylation among different cell types; we therefore analysed the cell type-enriched genes identified previously to have a first overview of the methylation profiles in different types of neural cells [67,68].

Mellén *et al.* [68] generated cell type-enriched gene lists including 922 Purkinje cell (PC), 2084 Bergmann glial cell (BG) and 986 granule neuronal cell (GC) enriched genes. These RNAs were compared to the cerebellar m⁶A-seq dataset resulting in 814, 704 and 1436 RNAs with detectable methylation in GCs, PCs and BGs, respectively (figure 4a). Notably, the proportion of methylated mRNAs in GCs was much higher than that in PCs or BGs. On average, methylated mRNAs in GCs contained more m⁶A peaks than those in the other two types of cells. We also evaluated their methylation levels by assessing the fold enrichment of all methylated peaks in each type of cells. In the cerebellum, methylation levels in GCs seemed to be the highest, while BGs displayed the lowest methylation levels (figure 4b). In the cerebral cortex, the neuronal cells (NCs), astrocytes (ASCs) and oligodendrocytes (ODCs) were also compared with regard to m⁶A methylation levels for the cell type-enriched RNAs. We found that NC-enriched RNAs had a higher proportion of methylation, more m⁶A peaks and higher methylation levels than ASC- and ODC-enriched RNAs (figure 4a,c). In figure 4d, the methylation status of several representative cell type-enriched mRNAs in the cerebellum and the cortex is shown in IGV plots.

The above results further confirmed the heterogeneity of RNA methylation not only in different brain regions but also in different types of neural cells. By comparing the methylation status of cell type-enriched genes, the NCs exhibited higher methylation levels than glial cells.

3.5. Distinct biological functions of commonly and specifically methylated genes

Morphogenesis and functional development of the brain are accomplished through multiple gene interaction networks in a spatio-temporal-specific manner. As a crucial post-transcriptional gene regulator, the functions of m⁶A marks in mRNA should be versatile in the brain. Considering the variation of RNA methylation in various brain regions, we next conducted GO analysis to explore the biological relevance of common and specific methylation in the cerebellum and the cerebral cortex (electronic supplementary material, tables S8–S11).

The top 3000 m⁶A peaks containing CMRs were selected for GO analysis. Owing to different methylation levels of common peaks in the two brain regions, the CMRs containing the top 3000 peaks were not identical, with only half of them overlapped (electronic supplementary material, figure S7a). However, in mouse cerebellum and cerebral cortex, these CMRs were enriched in very similar categories including transcriptional regulation, cell adhesion, axon guidance, synapse assembly and organization, suggesting that m⁶A is an essential modification involved in diverse physiological processes (figure 5a,b).

In contrast to common methylation, specific methylation was involved in different functional pathways in the two brain regions. Methylated RNAs were distributed throughout various organelles mainly including nucleus, cytoplasm, Golgi apparatus and membrane. The cerebellar SMR genes, located in the nucleus, cytoplasm and membrane, were mostly involved in transcriptional regulation, cell cycle, mRNA export, neuron maturation and so on (figure 5c). By contrast, cortical SMR genes were mainly detected in the dendrite, synapse and cell junction where chemical synapse transmission takes place. In line with their subcellular localization, GO annotation of the cortical SMR genes included synaptic transmission, memory, learning, axon guidance and ion transport (figure 5d). It is worth noting that in spite of the distinct functions, the majority of the SMRs (especially cerebellar SMRs) actually had similar expression levels between the two brain regions (electronic supplementary material, figure S7b), which further suggested a role of m⁶A methylation in regulating spatial-specific functions in mouse brain.

3.6. Hyper-methylation of FMRP target mRNAs

As revealed by GO functional annotation, CMRs and cortical SMRs were significantly enriched in the dendrite, synapse and cell junction, suggestive of the potential importance of m⁶A methylation in the synapse. We then examined the methylation status of the mRNAs encoding synaptic proteins by comparison with the mouse synaptic proteome [69,70]. As a result, 76.8% of mouse postsynaptic genes and 30% of pre-synaptic genes were detected with m⁶A RNA methylation (figure 6a,b), necessitating a requirement to explore the role of m⁶A marks in the synapse.

Local translational control is one of the key regulatory pathways for synaptic transmission; improper translational control will lead to synaptic dysfunction and subsequent cognitive disorders [71,72]. Fragile X syndrome (FXS) is such a kind of inherited disease characterized by intellectual disability and caused by *Fmr1* gene deletion or mutation, even though the mechanism is still under debate [73]. Fragile X mental retardation protein (FMRP), encoded by the *Fmr1* gene, regulates local protein translation in the synapse via its highly selective interaction with mRNAs. Various efforts have been made aiming to elucidate how FMRP recognizes its target mRNAs. Interestingly, FMRP-binding motifs on mRNAs (GGA, GAC, ACU) are highly similar to the consensus sequence of m⁶A methylation [74,75]. We then examined the possibility whether FMRP target mRNAs could be m⁶A methylated. Strikingly, among the 842 FMRP target mRNAs identified in mouse brain [76], 800 mRNAs were methylated in the cerebellum (95%) and 811 in the cortex (96%) (figure 6c). The numbers of m⁶A peaks in the methylated FMRP target mRNAs were much higher than the average level in all methylated mRNAs. Similar to the FMRP-binding sites in mRNAs, these peaks were mostly enriched in CDS regions, followed by the stop codon and the 3'UTR (figure 6d). Importantly, the median methylation levels of the methylated FMRP targets were considerably higher than that of all methylated mRNAs in both the cerebellum and the cortex (figure 6e). These findings implied that the m⁶A marks, especially those in the CDS regions, were most probably involved in the FMRP–RNA interactions.

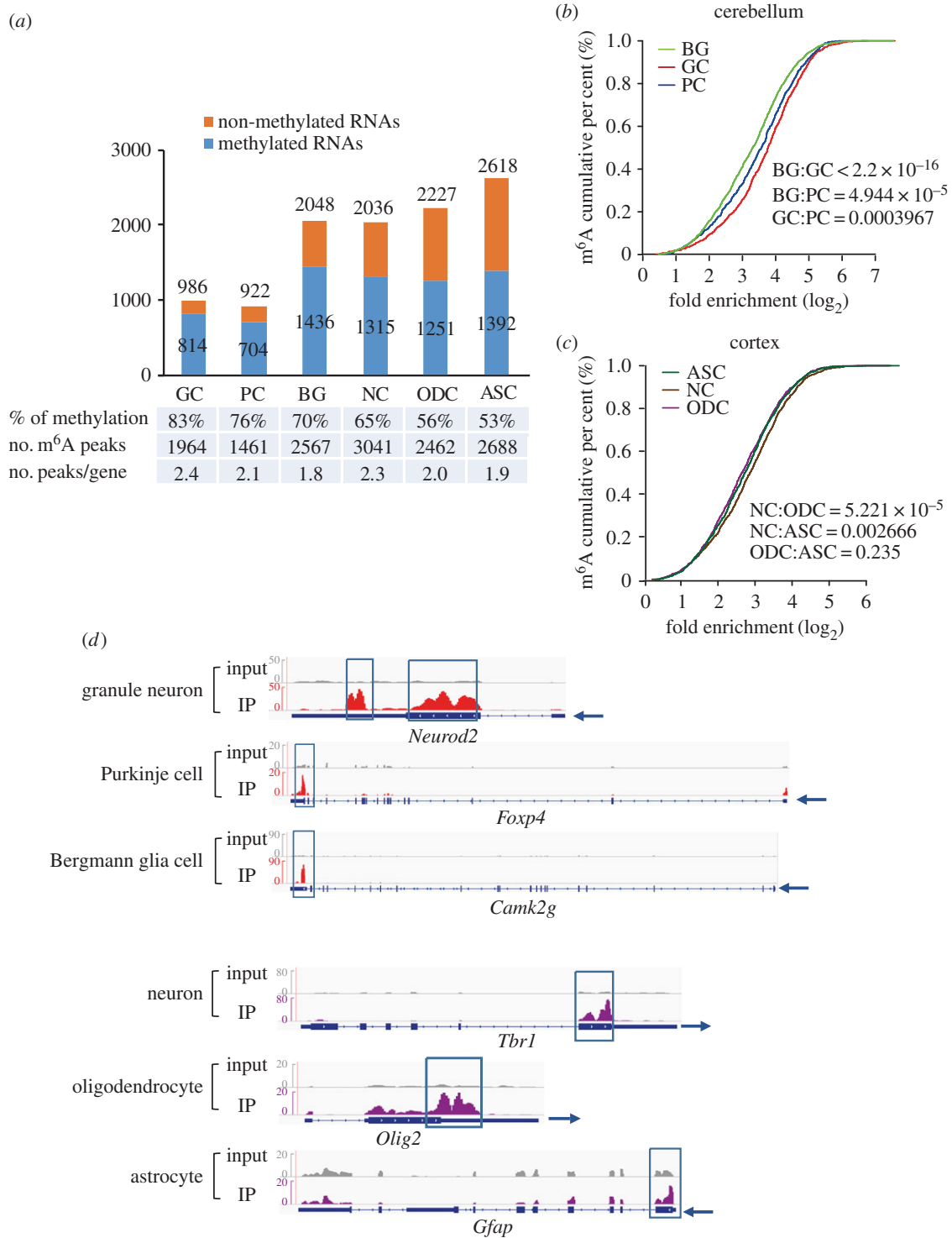


Figure 4. Universal RNA methylation in different types of neural cells. (a) Column charts showing the methylation status of different cell type-enriched genes in the cerebellum and the cortex. GC, granule neuronal cell; PC, Purkinje cell; BG, Bergmann glia cell; NC, neuronal cell; ODC, oligodendrocyte; ASC, astrocyte. The numbers of cell type-enriched genes are shown above each column; the numbers of methylated genes among those cell type-enriched genes are shown in the column. (b,c) Cumulative distribution function of log₂-fold enrichment of m⁶A peaks in three kinds of cell type-enriched genes in mouse cerebellum (b) or in mouse cerebral cortex (c). (d) IGV plots showing the methylation status of representative cell type-enriched genes in the cerebellum and the cortex. The grey reads are from non-IP control (input) libraries; red and purple reads are from m⁶A-IP libraries of mouse cerebellum and cerebral cortex, respectively. Arrows show the direction of transcription. Y-axis represents the normalized numbers of reads count. Positions of m⁶A peaks are highlighted in the blue box.

4. Discussion

Neural development is a complex process that follows a strict spatio-temporal pattern of organization, in which both genetic and epigenetic regulators undergo tightly regulated changes [77–79]. In this study, we provided the first region-specific m⁶A RNA methylation map and explored how it correlates

with the region-specific gene regulation in mouse cerebellum and cerebral cortex. Our results revealed several novel insights regarding the nature of m⁶A methylation in the brain. First, RNA methylation levels in mouse cerebellum are generally higher than those in the cerebral cortex. Second, heterogeneity of RNA methylation exists in different brain regions and different types of neural cells including the RNAs that are

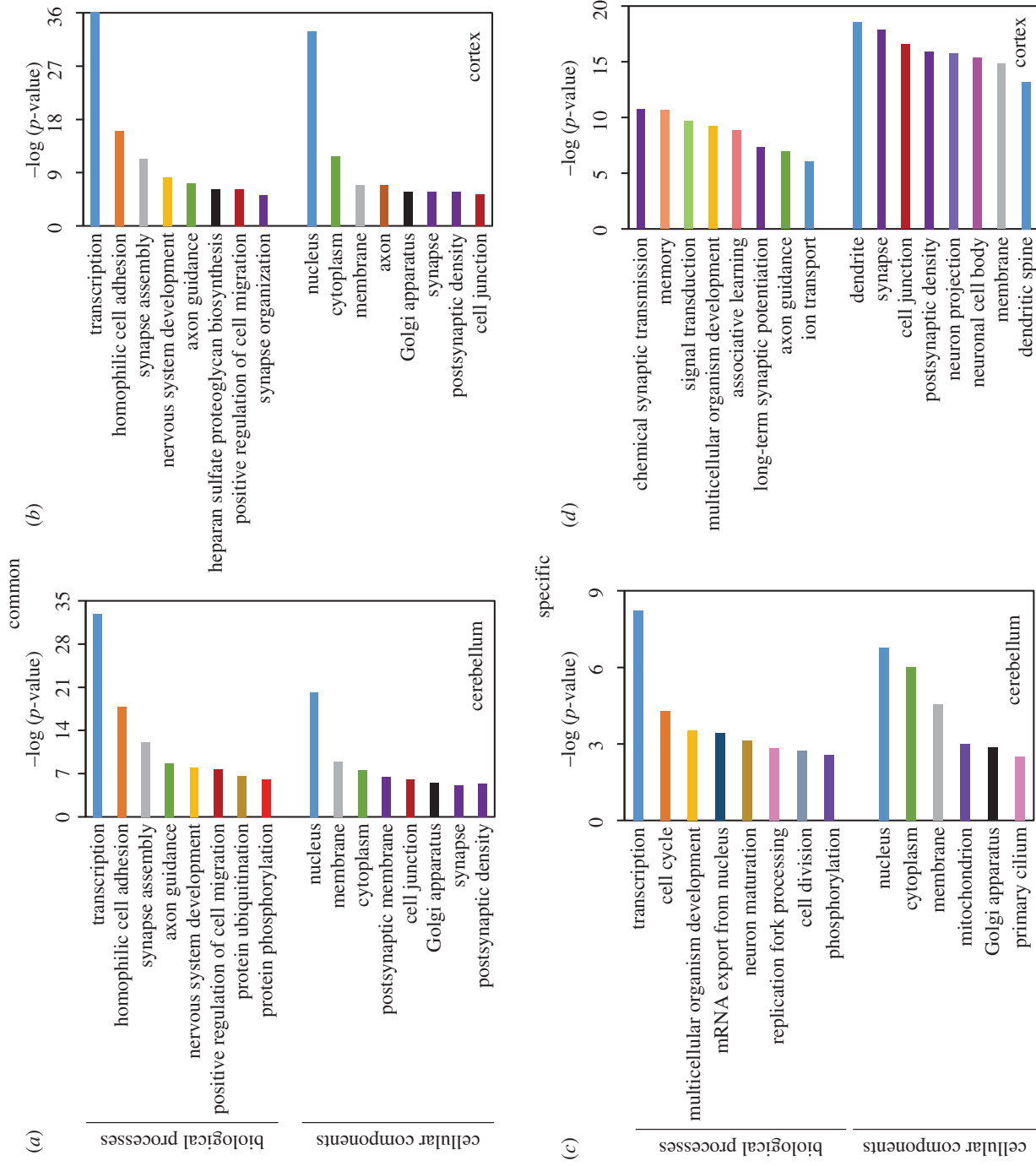


Figure 5. GO analysis of commonly and specifically methylated genes in mouse cerebellum and cerebral cortex. (a,b) GO functional analysis of the top 3000 m₆A peaks in mouse cerebellum (a) and cerebral cortex (b). (c,d) GO functional analysis of cerebellar (c) and cortical (d) specifically methylated genes.

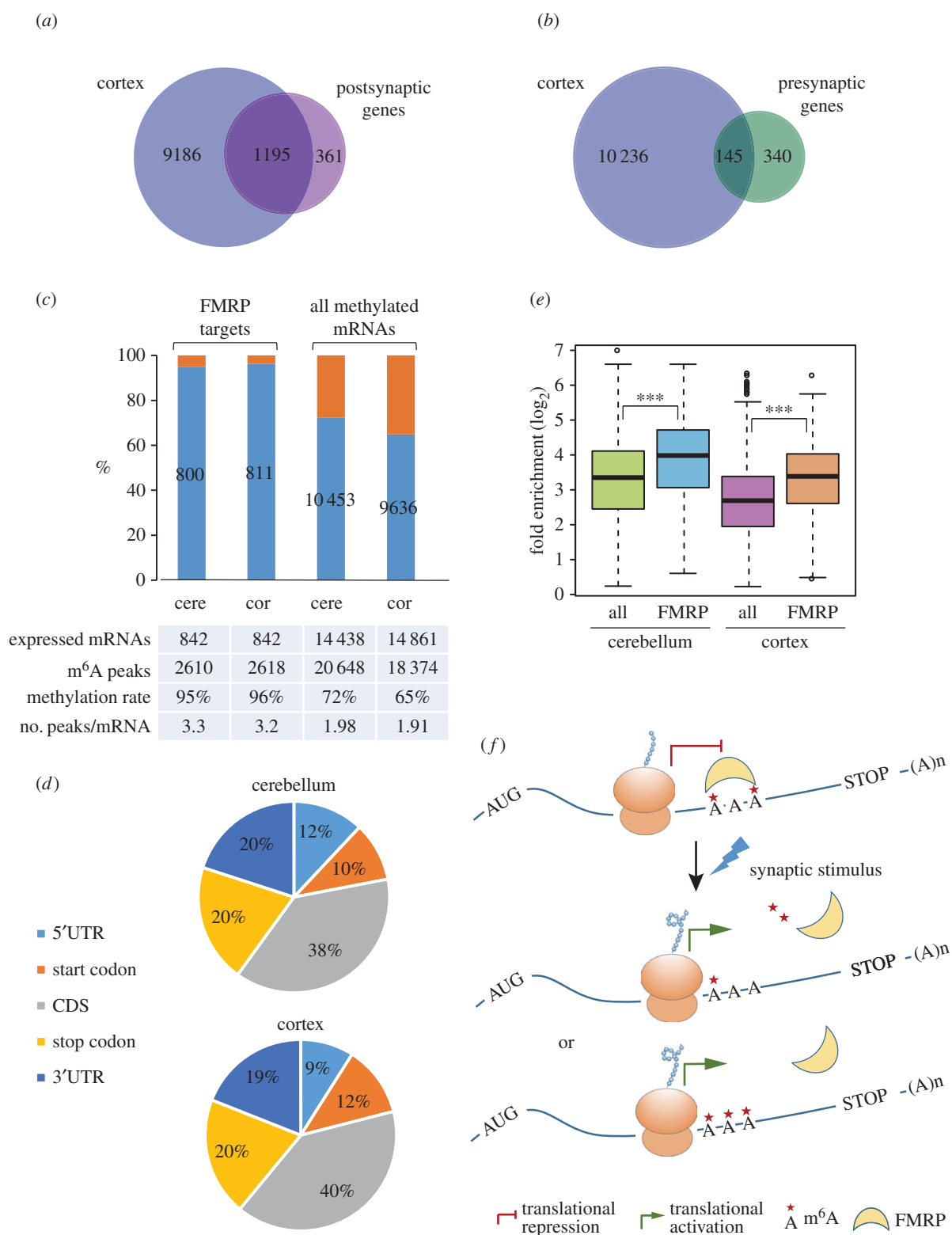


Figure 6. Methylation status of mouse synaptic mRNAs and FMRP target mRNAs in the mouse brain. (a,b) Venn diagrams showing the overlap between mouse cortical methylated genes and the genes encoding postsynaptic (a) or presynaptic proteins (b). (c) Column charts showing the methylation status of FMRP target mRNAs in comparison with all methylated mRNAs in mouse cerebellum and cerebral cortex. Orange bars indicate the unmethylated FMRP target mRNAs. The numbers on blue bars indicate the amount of methylated RNAs in each sample. (d) Pie charts showing the distribution of m⁶A peaks in methylated FMRP target mRNAs in mouse cerebellum and cerebral cortex. (e) Box plots showing the median methylation levels of FMRP target mRNAs in comparison with all methylated genes in mouse cerebellum and cerebral cortex, respectively. (f) Proposed model of the role of m⁶A RNA methylation in FMRP-induced translational repression. The target mRNAs are maintained at an appropriate RNA methylation level to be recognized by FMRP and enter a translational repression state via ribosome stalling. Upon relevant synaptic stimulus, mRNA methylation is altered, resulting from changed expression of one or more kinds of m⁶A writer, eraser or reader genes. Either increase or decrease in mRNA methylation may cause the dissociation of FMRP from target RNAs and then enable the ribosome elongation to reactivate translation. The one, two or three asterisks represent decreased, appropriate and increased methylation levels.

methylated, their methylation levels and the methylation sites. Third, common and region-specific methylation have different preferences for methylation site selection and thereby different

impacts on their biological functions. Last, our results also suggested that m⁶A methylation is likely to be used for selective recognition of target mRNAs by FMRP in the synapse.

RNA methylation mainly contributes to fine-tuning of gene regulation and is sensitive to experimental conditions. Therefore, instead of cell lines, the *in vivo* model system is better to be used to address the dynamics and biological functions of RNA methylation. We have observed higher expression of methyltransferases and demethylases in mouse cerebellum than in mouse cerebral cortex. Accordingly, the cerebellum contained more methylated RNAs with higher methylation levels. Through comparative analysis between the two regions, genes were divided into those whose mRNAs were methylated in both brain regions (CMRs), and those with specific methylation either in the cerebellum or the cortex (SMRs). m⁶A methylation is a fundamental requirement for CMRs to exert their functions in various physiological processes, but specific methylation is only needed on specified occasions; therefore, the methylation levels of CMRs are significantly higher than those of SMRs. Apart from its complex anatomical structure, the brain also contains a multitude of cell types, rendering interpretation of their specific functions a challenge [80]. By comparing the methylation status of the cell type-enriched RNAs [67,68], we found that the RNA methylation level in neurons was higher than that in glia, indicating a more important role of m⁶A in neurons. Taken together, in order to precisely characterize m⁶A methylation in the brain, regional and cellular heterogeneity have to be taken into consideration. In addition, how this region specificity of m⁶A methylation is achieved awaits further investigation.

For the first time, we reported a significant enrichment of cerebellum-specific m⁶A sites at start codons, and cortex-specific m⁶A sites in the CDS. Of note, due to the heterogeneity of RNA methylation across brain regions, the region-specific features of RNA methylation may be masked if the whole brain were to be analysed altogether. Enrichment of m⁶A at start codons has been previously observed in *Arabidopsis thaliana* and rice [81–83], indicating the evolutionary conservation of such a kind of distribution. Besides m⁶A, m¹A is another type of RNA modification enriched at start codons, which positively correlated with translation efficiency and protein expression levels [43,45]. Given the reported functions of m⁶A in translational control [10–12,84], we propose that m⁶A methylation at the start codon may be used for mRNA scanning for AUG recognition in highly metabolic active neurons [85]; however, this has to be confirmed with experimental evidence. In contrast to cerebellum-specific methylation sites, cortex-specific methylation sites are mostly detected in the CDS. Methylation analysis of FMRP target mRNAs indicates that the m⁶A marks in the CDS is probably used for selective recognition of mRNAs by FMRP.

As m⁶A modification can affect RNA structure and RNA–protein interactions, clustering of m⁶A peaks in different locations implies the versatile functions mediated via m⁶A marks. A prominent finding is that CMR genes and cortical SMR genes are enriched in the dendrites, synapses and cell junctions. Messenger RNAs localizing to these areas frequently undergo local protein translation in response to stimulus [86]. As protein translation levels correlate poorly with the mRNA abundance [87], there may exist alternative mechanisms for regulating local protein synthesis, one of which might be RNA modification. RNA m⁵C methyltransferase NSUN2 partially co-localized with FMRP, and the role of m⁵C RNA methylation in local protein translation

was investigated [88]. As a result, 5.3% of postsynaptic genes, 1.9% of presynaptic genes and 10% of FMRP target mRNAs were detected with m⁵C methylation. In contrast to m⁵C, we identified that m⁶A methylation occurred at a majority of synaptic RNAs and FMRP target mRNAs with particularly high methylation levels. Moreover, in line with the fact that FMRP prefers to bind the CDS region of target mRNAs, we also observed an enrichment of the m⁶A peaks of FMRP target mRNAs in the CDS region. Strikingly, the binding motifs of FMRP protein identified from several independent studies are highly similar to the consensus sequence of m⁶A methylation, among which A appears to be the most conserved site [74,75]. Further experimental investigation, such as single-nucleotide resolution m⁶A profiling analysis and FMRP PAR-CLIP, will be necessary to determine whether FMRP is a direct m⁶A-binding protein. Based on our observation in mouse cerebellum and cerebral cortex, we deduce that m⁶A methylation is probably involved in the FMRP translation repression mechanism, and propose a dynamic model of m⁶A modification in regulating local protein translation in the synapse. As illustrated in figure 6f, mRNA methylation is maintained in a proper balance to be recognized by the FMRP. Through m⁶A-mediated RNA–protein interaction, FMRP represses mRNA translation via stalling ribosomal translocation. Upon physiological synaptic stimuli, one or more kinds of m⁶A-related genes may be activated and may lead to an alteration in target mRNA methylation, which probably interferes with the FMRP–RNA interaction. Finally, FMRP is released from its target mRNA and protein translation is reinitiated. It is worth noting that the mechanism of synaptic signalling in different locations might vary a lot in response to different stimuli. The m⁶A peaks in FMRP target mRNAs located in the CDS region, stop codon and 3'UTR regions may participate in synaptic signalling in different ways. Hence, more detailed *in vivo* investigation is needed to ascertain the role of m⁶A in FMRP-mediated local protein translation in a context-dependent manner.

Absence or dysfunction of *Fmr1* gene causes loss of inhibitory functions of its target RNAs and results in excessive protein synthesis, which is one of the main causes of fragile X syndrome. Accordingly, the high methylation level of FMRP target mRNAs observed in this study implies that imbalanced RNA m⁶A methylation resulting from the defect in any of the m⁶A-related genes may also be a causative factor of intellectual disorder. In support of our findings, FTO was detected in the dendrites and near-dendritic spines of the mouse brain. Li *et al.* [35] also observed impaired learning and memory in targeted FTO knockout mice. Pathophysiological stimulation, such as transient contextual fear exposure, caused a significant decrease in FTO expression and an increase in m⁶A levels of mRNA in synapses [34]. Furthermore, *in situ* FTO depletion or FTO knock-down resulted in increased m⁶A methylation and enhanced memory formation in both mouse hippocampus and prefrontal cortex [34,89]. Recently, an SNP in the *ALKBH5* gene was identified in association with major mental disorders in the Chinese Han population [90]. *FTO* genetic variants were also reported associated with a high risk of Alzheimer's disease and impaired brain functions [91,92]. Therefore, it is of paramount importance to characterize m⁶A RNA methylation in greater detail, with much attention to its spatio-temporal specificity and cellular heterogeneity in the brain.

Nevertheless, it should be noted that, despite the several novel insights obtained, there are several limitations in this study. First, the common and specific methylation described above does not reflect the situation of the whole mouse brain because only the cerebellum and the cerebral cortex were included for comparison. Second, the m⁶A-seq analysis used in this study cannot tell the exact location of methylation sites at base level, therefore m⁶A analysis of single-nucleotide resolution will be necessary in order to precisely evaluate the role of m⁶A at specified methylation sites. Third, the RNA methylation in various types of cells as evaluated only with the cell type-enriched genes, thus the information of the low-abundance but highly methylated RNAs was missing. In addition, because we used a mixture of multiple types of cells for m⁶A-seq, the methylation status of each gene in different cells cannot be characterized here. Therefore, to thoroughly study the heterogeneity of RNA methylation and related functions, there is a pressing need to develop an accurate, sensitive and quantitative method for m⁶A analysis.

5. Conclusion

In summary, we analysed the region-specific methylation profiles and characterized their functions in mouse cerebellum and cerebral cortex. Our results imply that RNA methylation exhibits different characteristics across different brain regions or different types of neural cells. As a representative epitranscriptomic mark, m⁶A is a newly identified element in the region-specific gene regulatory network in

the mouse brain. Elucidation of an m⁶A-dependent regulatory network in the brain should greatly facilitate our understanding of brain development and help unravel the aetiology of neurological diseases, which in turn might be able to offer novel diagnostic or therapeutic targets in the future.

Ethics. All animal experiments and euthanasia were approved and performed in accordance with the guidelines of the Animal Care and Use Committee of IBMS/PUMC.

Data accessibility. The datasets supporting the conclusions of this article are available in the Genome Sequence Archive (GSA) of BIG Data Center, Beijing Institute of Genomics (BIG), Chinese Academy of Sciences and are publicly accessible at <http://gsa.big.ac.cn> (Accession no. PRJCA000272).

Authors' contributions. C.M. performed the experiments with the assistance of H.X. and Z.S. L.H. performed bioinformatic analysis with the assistance of Z.W., M.C. and Z.Z.W. S.S. and Z.Y. participated in the design of the study. N.Y. and T.W.M. conceived and supervised the project. All authors read and approved the final manuscript.

Competing interests. The authors declare that they have no competing interests.

Funding. This work was supported by the National Natural Science Foundation of China (31471288 to N.Y., 31471343 to T.W.-M.), the CAMS Innovation Fund for Medical Sciences (CIFMS) (2016-I2M-1004 to N.Y.) and the Fundamental Research Funds for the Central Universities (33320140041 to N.Y., 2014199 to T.W.-M.).

Acknowledgements. We thank the Center of Experimental Animal Research at the IBMS/CAMS for all animal care. We express our thanks to Dr B. Huang for his critical discussion. We are indebted to the sequencing core facility of Beijing Institute of Genomics, Chinese Academy of Sciences for sequencing.

References

- Liu N, Dai Q, Zheng G, He C, Parisien M, Pan T. 2015 N⁶-methyladenosine-dependent RNA structural switches regulate RNA–protein interactions. *Nature* **518**, 560–564. (doi:10.1038/nature14234)
- Niu Y, Zhao X, Wu YS, Li MM, Wang XJ, Yang YG. 2013 N⁶-methyl-adenosine (m⁶A) in RNA: an old modification with a novel epigenetic function. *Genomics Proteomics Bioinform.* **11**, 8–17. (doi:10.1016/j.gpb.2012.12.002)
- Fu Y, Dominissini D, Rechavi G, He C. 2014 Gene expression regulation mediated through reversible m⁶A RNA methylation. *Nat. Rev. Genet.* **15**, 293–306. (doi:10.1038/nrg3724)
- Xiao W *et al.* 2016 Nuclear m⁶A reader YTHDC1 regulates mRNA splicing. *Mol. Cell.* **61**, 507–519. (doi:10.1016/j.molcel.2016.01.012)
- Roundtree IA, He C. 2016 Nuclear m⁶A reader YTHDC1 regulates mRNA splicing. *Trends Genet.* **32**, 320–321. (doi:10.1016/j.tig.2016.03.006)
- Zheng G *et al.* 2013 ALKBH5 is a mammalian RNA demethylase that impacts RNA metabolism and mouse fertility. *Mol. Cell.* **49**, 18–29. (doi:10.1016/j.molcel.2012.10.015)
- Alarcon CR, Lee H, Goodarzi H, Halberg N, Tavazoie SF. 2015 N⁶-methyladenosine marks primary microRNAs for processing. *Nature* **519**, 482–485. (doi:10.1038/nature14281)
- Alarcon CR, Goodarzi H, Lee H, Liu X, Tavazoie S, Tavazoie SF. 2015 HNRNPA2B1 is a mediator of m⁶A-dependent nuclear RNA processing events. *Cell* **162**, 1299–1308. (doi:10.1016/j.cell.2015.08.011)
- Choi J *et al.* 2016 N⁶-methyladenosine in mRNA disrupts tRNA selection and translation-elongation dynamics. *Nat. Struct. Mol. Biol.* **23**, 110–115. (doi:10.1038/nsmb.3148)
- Zhou J, Wan J, Gao X, Zhang X, Jaffrey SR, Qian SB. 2015 Dynamic m⁶A mRNA methylation directs translational control of heat shock response. *Nature* **526**, 591–594. (doi:10.1038/nature15377)
- Wang X *et al.* 2015 N⁶-methyladenosine modulates messenger RNA translation efficiency. *Cell* **161**, 1388–1399. (doi:10.1016/j.cell.2015.05.014)
- Meyer KD, Patil DP, Zhou J, Zinoviev A, Skabkin MA, Elemento O, Pestova TV, Qian SB, Jaffrey SR. 2015 5' UTR m⁶A promotes cap-independent translation. *Cell* **163**, 999–1010. (doi:10.1016/j.cell.2015.10.012)
- Shi H, Wang X, Lu Z, Zhao BS, Ma H, Hsu PJ, Liu C, He C. 2017 YTHDF3 facilitates translation and decay of N⁶-methyladenosine-modified RNA. *Cell Res.* **27**, 315–328. (doi:10.1038/cr.2017.15)
- Li A *et al.* 2017 Cytoplasmic m⁶A reader YTHDF3 promotes mRNA translation. *Cell Res.* **27**, 444–447. (doi:10.1038/cr.2017.10)
- Slobodin B, Han R, Calderone V, Vrieling JA, Loayza-Puch F, Elkon R, Agami R. 2017 Transcription impacts the efficiency of mRNA translation via co-transcriptional N⁶-adenosine methylation. *Cell* **169**, 326–337. (doi:10.1016/j.cell.2017.03.031)
- Wang X *et al.* 2014 N⁶-methyladenosine-dependent regulation of messenger RNA stability. *Nature* **505**, 117–120. (doi:10.1038/nature12730)
- Du H, Zhao Y, He J, Zhang Y, Xi H, Liu M, Ma J, Wu L. 2016 YTHDF2 destabilizes m⁶A-containing RNA through direct recruitment of the CCR4-NOT deadenylase complex. *Nat. Commun.* **7**, 12626. (doi:10.1038/ncomms12626)
- Liu N, Pan T. 2016 N⁶-methyladenosine-encoded epitranscriptomics. *Nat. Struct. Mol. Biol.* **23**, 98–102. (doi:10.1038/nsmb.3162)
- Patil DP, Chen CK, Pickering BF, Chow A, Jackson C, Guttman M, Jaffrey SR. 2016 m⁶A RNA methylation promotes XIST-mediated transcriptional repression. *Nature* **537**, 369–373. (doi:10.1038/nature19342)
- Shah JC, Clancy MJ. 1992 IME4, a gene that mediates MAT and nutritional control of meiosis in *Saccharomyces cerevisiae*. *Mol. Cell Biol.* **12**, 1078–1086. (doi:10.1128/MCB.12.3.1078)

21. Zhong S, Li H, Bodi Z, Button J, Vespa L, Herzog M, Fray RG. 2008 MTA is an *Arabidopsis* messenger RNA adenosine methylase and interacts with a homolog of a sex-specific splicing factor. *Plant Cell* **20**, 1278–1288. (doi:10.1105/tpc.108.058883)
22. Ping XL *et al.* 2014 Mammalian WTAP is a regulatory subunit of the RNA N⁶-methyladenosine methyltransferase. *Cell Res.* **24**, 177–189. (doi:10.1038/cr.2014.3)
23. Hongay CF, Orr-Weaver TL. 2011 *Drosophila* inducer of Meiosis 4 (IME4) is required for Notch signaling during oogenesis. *Proc. Natl Acad. Sci. USA* **108**, 14 855–14 860. (doi:10.1073/pnas.1111577108)
24. Liu J *et al.* 2014 A METTL3-METTL14 complex mediates mammalian nuclear RNA N⁶-adenosine methylation. *Nat. Chem. Biol.* **10**, 93–95. (doi:10.1038/nchembio.1432)
25. Wang Y, Li Y, Toth JI, Petroski MD, Zhang Z, Zhao JC. 2014 N⁶-methyladenosine modification destabilizes developmental regulators in embryonic stem cells. *Nat. Cell Biol.* **16**, 191–198. (doi:10.1038/ncb2902)
26. Aguilo F *et al.* 2015 Coordination of m⁶A mRNA methylation and gene transcription by ZFP217 regulates pluripotency and reprogramming. *Cell Stem Cell* **17**, 689–704. (doi:10.1016/j.stem.2015.09.005)
27. Chen T *et al.* 2015 m⁶A RNA methylation is regulated by microRNAs and promotes reprogramming to pluripotency. *Cell Stem Cell* **16**, 289–301. (doi:10.1016/j.stem.2015.01.016)
28. Geula S *et al.* 2015 Stem cells. m⁶A mRNA methylation facilitates resolution of naive pluripotency toward differentiation. *Science* **347**, 1002–1006. (doi:10.1126/science.1261417)
29. Batista PJ *et al.* 2014 m⁶A RNA modification controls cell fate transition in mammalian embryonic stem cells. *Cell Stem Cell* **15**, 707–719. (doi:10.1016/j.stem.2014.09.019)
30. Fustin JM *et al.* 2013 RNA-methylation-dependent RNA processing controls the speed of the circadian clock. *Cell* **155**, 793–806. (doi:10.1016/j.cell.2013.10.026)
31. Jia G *et al.* 2011 N⁶-methyladenosine in nuclear RNA is a major substrate of the obesity-associated FTO. *Nat. Chem. Biol.* **7**, 885–887. (doi:10.1038/nchembio.687)
32. Zhao X *et al.* 2014 FTO-dependent demethylation of N⁶-methyladenosine regulates mRNA splicing and is required for adipogenesis. *Cell Res.* **24**, 1403–1419. (doi:10.1038/cr.2014.151)
33. Hess ME *et al.* 2013 The fat mass and obesity associated gene (*Fto*) regulates activity of the dopaminergic midbrain circuitry. *Nat. Neurosci.* **16**, 1042–1048. (doi:10.1038/nn.3449)
34. Widagdo J *et al.* 2016 Experience-dependent accumulation of N⁶-methyladenosine in the prefrontal cortex is associated with memory processes in mice. *J. Neurosci.* **36**, 6771–6777. (doi:10.1523/JNEUROSCI.4053-15.2016)
35. Li L *et al.* 2017 Fat mass and obesity-associated (FTO) protein regulates adult neurogenesis. *Hum. Mol. Genet.* **26**, 2398–2411. (doi:10.1093/hmg/ddx128)
36. Yao B, Christian KM, He C, Jin P, Ming GL, Song H. 2016 Epigenetic mechanisms in neurogenesis. *Nat. Rev. Neurosci.* **17**, 537–549. (doi:10.1038/nrn.2016.70)
37. Guo JU *et al.* 2011 Neuronal activity modifies the DNA methylation landscape in the adult brain. *Nat. Neurosci.* **14**, 1345–1351. (doi:10.1038/nn.2900)
38. Hirabayashi Y, Suzuki N, Tsuboi M, Endo TA, Toyoda T, Shinga J, Koseki H, Vidal M, Gotoh Y. 2009 Polycomb limits the neurogenic competence of neural precursor cells to promote astrogenic fate transition. *Neuron* **63**, 600–613. (doi:10.1016/j.neuron.2009.08.021)
39. Lim DA, Huang Y-C, Swigut T, Mirick AL, Garcia-Verdugo JM, Wysocka J, Ernst P, Alvarez-Buylla A. 2009 Chromatin remodelling factor Mll1 is essential for neurogenesis from postnatal neural stem cells. *Nature* **458**, 529–533. (doi:10.1038/nature07726)
40. Ramos AD, Diaz A, Nellore A, Delgado RN, Park KY, Gonzales-Roybal G, Oldham MC, Song JS, Lim DA. 2013 Integration of genome-wide approaches identifies lncRNAs of adult neural stem cells and their progeny *in vivo*. *Cell Stem Cell* **12**, 616–628. (doi:10.1016/j.stem.2013.03.003)
41. Roundtree IA, He C. 2016 RNA epigenetics—chemical messages for posttranscriptional gene regulation. *Curr. Opin. Chem. Biol.* **30**, 46–51. (doi:10.1016/j.cbpa.2015.10.024)
42. Squires JE, Patel HR, Nousch M, Sibbritt T, Humphreys DT, Parker BJ, Suter CM, Preiss T. 2012 Widespread occurrence of 5-methylcytosine in human coding and non-coding RNA. *Nucleic Acids Res.* **40**, 5023–5033. (doi:10.1093/nar/gks144)
43. Dominissini D *et al.* 2016 The dynamic N¹-methyladenosine methylome in eukaryotic messenger RNA. *Nature* **530**, 441–446. (doi:10.1038/nature16998)
44. Liu J, Jia G. 2014 Methylation modifications in eukaryotic messenger RNA. *J. Genet. Genomics.* **41**, 21–33. (doi:10.1016/j.jgg.2013.10.002)
45. Li X, Xiong X, Wang K, Wang L, Shu X, Ma S, Yi C. 2016 Transcriptome-wide mapping reveals reversible and dynamic N¹-methyladenosine methylome. *Nat. Chem. Biol.* **12**, 311–316. (doi:10.1038/nchembio.2040)
46. Nainar S, Marshall PR, Tyler CR, Spitale RC, Bredy TW. 2016 Evolving insights into RNA modifications and their functional diversity in the brain. *Nat. Neurosci.* **19**, 1292–1298. (doi:10.1038/nn.4378)
47. Zhang S *et al.* 2017 m⁶A demethylase ALKBH5 maintains tumorigenicity of glioblastoma stem-like cells by sustaining FOXM1 expression and cell proliferation program. *Cancer Cell* **31**, 591–606. (doi:10.1016/j.ccell.2017.02.013)
48. Meyer KD, Saletore Y, Zumbo P, Elemento O, Mason CE, Jaffrey SR. 2012 Comprehensive analysis of mRNA methylation reveals enrichment in 3' UTRs and near stop codons. *Cell* **149**, 1635–1646. (doi:10.1016/j.cell.2012.05.003)
49. LoVerso PR, Cui F. 2016 Cell type-specific transcriptome profiling in mammalian brains. *Front. Biosci.* **21**, 973–985. (doi:10.2741/4434)
50. Kessler NJ, Van Baak TE, Baker MS, Laritsky E, Coarfa C, Waterland RA. 2016 CpG methylation differences between neurons and glia are highly conserved from mouse to human. *Hum. Mol. Genet.* **25**, 223–232. (doi:10.1093/hmg/ddv459)
51. Spijker S. 2011 Dissection of rodent brain regions. In *Neuroproteomics* (ed. KW Li), pp. 13–26. New York, NY: Humana Press.
52. Kim D, Pertea G, Trapnell C, Pimentel H, Kelley R, Salzberg SL. 2013 TopHat2: accurate alignment of transcriptomes in the presence of insertions, deletions and gene fusions. *Genome Biol.* **14**, R36. (doi:10.1186/gb-2013-14-4-r36)
53. Trapnell C, Pachter L, Salzberg SL. 2009 TopHat: discovering splice junctions with RNA-Seq. *Bioinformatics* **25**, 1105–1111. (doi:10.1093/bioinformatics/btp120)
54. Trapnell C *et al.* 2012 Differential gene and transcript expression analysis of RNA-seq experiments with TopHat and Cufflinks. *Nat. Protoc.* **7**, 562–578. (doi:10.1038/nprot.2012.016)
55. Trapnell C, Williams BA, Pertea G, Mortazavi A, Kwan G, van Baren MJ, Salzberg SL, Wold BJ, Pachter L. 2010 Transcript assembly and quantification by RNA-Seq reveals unannotated transcripts and isoform switching during cell differentiation. *Nat. Biotechnol.* **28**, 511–515. (doi:10.1038/nbt.1621)
56. Meng J, Cui X, Rao MK, Chen Y, Huang Y. 2013 Exome-based analysis for RNA epigenome sequencing data. *Bioinformatics* **29**, 1565–1567. (doi:10.1093/bioinformatics/btt171)
57. Liu L, Zhang SW, Zhang YC, Liu H, Zhang L, Chen R, Huang Y, Meng J. 2015 Decomposition of RNA methylome reveals co-methylation patterns induced by latent enzymatic regulators of the epitranscriptome. *Mol. Biosyst.* **11**, 262–274. (doi:10.1039/c4mb00604f)
58. Quinlan AR, Hall IM. 2010 BEDTools: a flexible suite of utilities for comparing genomic features. *Bioinformatics* **26**, 841–842. (doi:10.1093/bioinformatics/btq033)
59. Heinz S *et al.* 2010 Simple combinations of lineage-determining transcription factors prime cis-regulatory elements required for macrophage and B cell identities. *Mol. Cell.* **38**, 576–589. (doi:10.1016/j.molcel.2010.05.004)
60. Zhang Y *et al.* 2008 Model-based analysis of ChIP-Seq (MACS). *Genome Biol.* **9**, R137. (doi:10.1186/gb-2008-9-9-r137)
61. Dominissini D, Moshitch-Moshkovitz S, Salmon-Divon M, Amariglio N, Rechavi G. 2013 Transcriptome-wide mapping of N⁶-methyladenosine by m⁶A-seq based on immunocapturing and massively parallel sequencing. *Nat. Protoc.* **8**, 176–189. (doi:10.1038/nprot.2012.148)
62. Dominissini D *et al.* 2012 Topology of the human and mouse m⁶A RNA methylomes revealed by m⁶A-seq. *Nature* **485**, 201–206. (doi:10.1038/nature11112)

63. Huang da W, Sherman BT, Lempicki RA. 2009 Systematic and integrative analysis of large gene lists using DAVID bioinformatics resources. *Nat. Protoc.* **4**, 44–57. (doi:10.1038/nprot.2008.211)
64. Mauer J *et al.* 2017 Reversible methylation of m⁶A in the 5' cap controls mRNA stability. *Nature* **541**, 371–375. (doi:10.1038/nature21022)
65. Molinie B *et al.* 2016 m⁶A-LAIC-seq reveals the census and complexity of the m⁶A epitranscriptome. *Nat. Methods* **13**, 692. (doi:10.1038/nmeth.3898)
66. Linder B, Grozhik AV, Olarerin-George AO, Meydan C, Mason CE, Jaffrey SR. 2015 Single-nucleotide-resolution mapping of m⁶A and m⁶Am throughout the transcriptome. *Nat. Methods* **12**, 767–772. (doi:10.1038/nmeth.3453)
67. Cahoy JD *et al.* 2008 A transcriptome database for astrocytes, neurons, and oligodendrocytes: a new resource for understanding brain development and function. *J. Neurosci.* **28**, 264–278. (doi:10.1523/JNEUROSCI.4178-07.2008)
68. Mellen M, Ayata P, Dewell S, Kriaucionis S, Heintz N. 2012 MeCP2 binds to 5hmC enriched within active genes and accessible chromatin in the nervous system. *Cell* **151**, 1417–1430. (doi:10.1016/j.cell.2012.11.022)
69. Croning MD, Marshall MC, McLaren P, Armstrong JD, Grant SG. 2009 G2Cdb: the Genes to Cognition database. *Nucleic Acids Res.* **37**, D846–D851. (doi:10.1093/nar/gkn700)
70. Weingarten J *et al.* 2014 The proteome of the presynaptic active zone from mouse brain. *Mol. Cell Neurosci.* **59**, 106–118. (doi:10.1016/j.mcn.2014.02.003)
71. Iacoangeli A, Tiedge H. 2013 Translational control at the synapse: role of RNA regulators. *Trends Biochem. Sci.* **38**, 47–55. (doi:10.1016/j.tibs.2012.11.001)
72. Buffington SA, Huang W, Costa-Mattioli M. 2014 Translational control in synaptic plasticity and cognitive dysfunction. *Annu. Rev. Neurosci.* **37**, 17–38. (doi:10.1146/annurev-neuro-071013-014100)
73. Verkerk AJ *et al.* 1991 Identification of a gene (FMR-1) containing a CGG repeat coincident with a breakpoint cluster region exhibiting length variation in fragile X syndrome. *Cell* **65**, 905–914. (doi:10.1016/0092-8674(91)90397-H)
74. Suhl JA, Chopra P, Anderson BR, Bassell GJ, Warren ST. 2014 Analysis of FMRP mRNA target datasets reveals highly associated mRNAs mediated by G-quadruplex structures formed via clustered WGGG sequences. *Hum. Mol. Genet.* **23**, 5479–5491. (doi:10.1093/hmg/ddu272)
75. Anderson BR, Chopra P, Suhl JA, Warren ST, Bassell GJ. 2016 Identification of consensus binding sites clarifies FMRP binding determinants. *Nucleic Acids Res.* **44**, 6649–6659. (doi:10.1093/nar/gkw593)
76. Darnell JC *et al.* 2011 FMRP stalls ribosomal translocation on mRNAs linked to synaptic function and autism. *Cell* **146**, 247–261. (doi:10.1016/j.cell.2011.06.013)
77. Frank CL *et al.* 2015 Regulation of chromatin accessibility and Zic binding at enhancers in the developing cerebellum. *Nat. Neurosci.* **18**, 647–656. (doi:10.1038/nn.3995)
78. Szulwach KE *et al.* 2011 5-hmC-mediated epigenetic dynamics during postnatal neurodevelopment and aging. *Nat. Neurosci.* **14**, 1607–1616. (doi:10.1038/nn.2959)
79. Chou SJ, Wang C, Sintupisut N, Niou ZX, Lin CH, Li KC, Yeang CH. 2016 Analysis of spatial-temporal gene expression patterns reveals dynamics and regionalization in developing mouse brain. *Sci. Rep.* **6**, 19274. (doi:10.1038/srep19274)
80. Emery B, Barres BA. 2008 Unlocking CNS cell type heterogeneity. *Cell* **135**, 596–598. (doi:10.1016/j.cell.2008.10.031)
81. Li Y, Wang X, Li C, Hu S, Yu J, Song S. 2014 Transcriptome-wide N⁶-methyladenosine profiling of rice callus and leaf reveals the presence of tissue-specific competitors involved in selective mRNA modification. *RNA Biol.* **11**, 1180–1188. (doi:10.4161/rna.36281)
82. Luo GZ *et al.* 2014 Unique features of the m⁶A methylome in *Arabidopsis thaliana*. *Nat. Commun.* **5**, 5630. (doi:10.1038/ncomms6630)
83. Yue Y, Liu J, He C. 2015 RNA N⁶-methyladenosine methylation in post-transcriptional gene expression regulation. *Genes Dev.* **29**, 1343–1355. (doi:10.1101/gad.262766.115)
84. Zhou J, Rode KA, Qian SB. 2016 m⁶A: a novel hallmark of translation. *Cell Cycle* **15**, 309–310. (doi:10.1080/15384101.2015.1125240)
85. Hinnebusch AG. 2014 The scanning mechanism of eukaryotic translation initiation. *Annu. Rev. Biochem.* **83**, 779–812. (doi:10.1146/annurev-biochem-060713-035802)
86. Martin KC, Zukin RS. 2006 RNA trafficking and local protein synthesis in dendrites: an overview. *J. Neurosci.* **26**, 7131–7134. (doi:10.1523/JNEUROSCI.1801-06.2006)
87. Ingolia NT. 2014 Ribosome profiling: new views of translation, from single codons to genome scale. *Nat. Rev. Genet.* **15**, 205–213. (doi:10.1038/nrg3645)
88. Hussain S, Bashir ZI. 2015 The epitranscriptome in modulating spatiotemporal RNA translation in neuronal post-synaptic function. *Front. Cell Neurosci.* **9**, 420. (doi:10.3389/fncel.2015.00420)
89. Walters BJ, Mercaldo V, Gillon CJ, Yip M, Neve RL, Boyce FM, Frankland PW, Josselyn SA. 2017 The role of The RNA demethylase FTO (Fat Mass and Obesity-Associated) and mRNA methylation in hippocampal memory formation. *Neuropsychopharmacology* **42**, 1502–1510. (doi:10.1038/npp.2017.31)
90. Du T, Rao S, Wu L, Ye N, Liu Z, Hu H, Xiu J, Shen Y, Xu Q. 2015 An association study of the m⁶A genes with major depressive disorder in Chinese Han population. *J. Affect. Disorders* **183**, 279–286. (doi:10.1016/j.jad.2015.05.025)
91. Keller L, Xu W, Wang HX, Winblad B, Fratiglioni L, Graff C. 2011 The obesity related gene, FTO, interacts with APOE, and is associated with Alzheimer's Dis. risk: a prospective cohort study. *J. Alzheimer's Dis.* **23**, 461–469. (doi:10.3233/JAD-2010-101068)
92. Reitz C *et al.* 2012 Genetic variants in the Fat and Obesity Associated (FTO) gene and risk of Alzheimer's disease. *PLoS ONE* **7**, e50354. (doi:10.1371/journal.pone.0050354)